J. of Supercritical Fluids 107 (2016) 51–60

Contents lists available at ScienceDirect

The Journal of Supercritical Fluids

journal homepage: www.elsevier.com/locate/supflu

Tetracycline nanoparticles precipitation using supercritical and liquid CO_2 as antisolvents

Tae Jun Yoon, Won-Su Son, Hee Jeong Park, Bumjoon Seo, Taewan Kim, Youn-Woo Lee*

School of Chemical and Biological Engineering and Institute of Chemical Processes, Seoul National University, 1 Gwanak-ro, Gwanak-gu, Seoul 151-744, Republic of Korea

ARTICLE INFO

Article history:
Received 25 July 2015
Received in revised form 20 August 2015
Accepted 24 August 2015
Available online 28 August 2015

Keywords:
Precipitation with compressed fluid antisolvent (PCA)
Nanoparticle
Coalescence
Surface diffusion
Solvent/antisolvent interaction
Hansen solubility parameter (HSP)

ABSTRACT

Tetracycline has been obtained as amorphous agglomerates in the supercritical antisolvent process. This phenomenon has been postulated to occur due to weak solvent/antisolvent interaction. In order to verify the hypothesis and prevent the coalescence of nanoparticles, we micronized tetracycline hydrochloride using supercritical and liquid CO_2 in the precipitation with compressed fluid antisolvent process (PCA). PCA experiments were performed by varying temperature, pressure and initial concentration of the solution. SEM and BET were used to understand the coalescence behavior. Mean surface area (S_{BET}) of the precipitates from liquid conditions was 58.91 m^2/g, which was approximately two times higher than the mean surface area of the precipitates from supercritical conditions (S_{BET} = 29.98 m^2/g). Hansen distance (R), an indicator of solvent/antisolvent interaction, was used to understand the macroscopic phase behavior and solvent/antisolvent interactions. The result implied that both surface diffusion of the precipitates and solvent/antisolvent interactions affected the coalescence behavior. As a result, we successfully formulated tetracycline nanoparticles without extensive coalescence using liquid CO_2 as an antisolvent.

1. Introduction

Nanoparticles can be utilized in the field of pharmaceutical science due to high bioavailability and controlled release [1]. These characters depend on the physicochemical properties such as particle size, surface area and crystallinity. Thus, a variety of micronization processes such as spray drying, milling technologies and drowning-out crystallization have been developed to micronize pharmaceuticals. Among them, supercritical antisolvent (SAS) process is regarded as a promising technique to micronize pharmaceuticals without chemical degradation. This process features mild temperature, uses small amount of organic solvents and formulates ultrafine particles without additional drying process. Many kinds of pharmaceuticals have been successfully micronized in this process [2].

However, some of the pharmaceuticals have been obtained as coalesced or sintered particles [3–7]. The coalescence of the precipitates decreases the surface to volume ratio. This results in the decreased dissolution rate of poorly water-soluble drugs [5] and hampers the feasibility of various drug delivery routes such as direct cellular uptake of nanoparticles [8]. Therefore, it is essential to understand and control the coalescence behavior in the micronization process.

The coalescence mechanisms have been classified depending on the supramolecular structure of the precipitates; dissolution–precipitation and viscous flow mechanism. Highly ordered crystalline materials tend to coalesce by dissolution–precipitation. On the other hand, amorphous materials are inclined to coalesce due to viscous flow among the precipitates [9]. This dissimilarity between crystalline and amorphous materials originates from molecular mobility and free volume in the precipitates. Frenkel first suggested a general model to explain the coalescence of amorphous materials [10,11]. In this model, coalescence rate largely depends on the surface diffusion of the precipitates [12,13]. The diffusion coefficient (D) of the coalescence rate is related to the viscosity of the solid phase. Thus, the coalescence rate shows Arrhenius temperature dependence as: $D \propto \exp(-T_m/T)$ and rapidly increases when the process temperature (T) is higher than $0.75T_m$ [14].

This model can be utilized to understand the coalescence behavior in the SAS process. First, melting points (T_m) of some materials are known to be significantly depressed in supercritical CO_2 [5,7,15–17]. Furthermore, supercritical mixture of co-solvent and carbon dioxide decreases the melting point of the precipitates more

* Corresponding author. Tel.: +82 2 880 1883; fax: +82 2 883 9124.
E-mail address: ywlee@snu.ac.kr (Y.-W. Lee).

http://dx.doi.org/10.1016/j.supflu.2015.08.014
0896-8446/

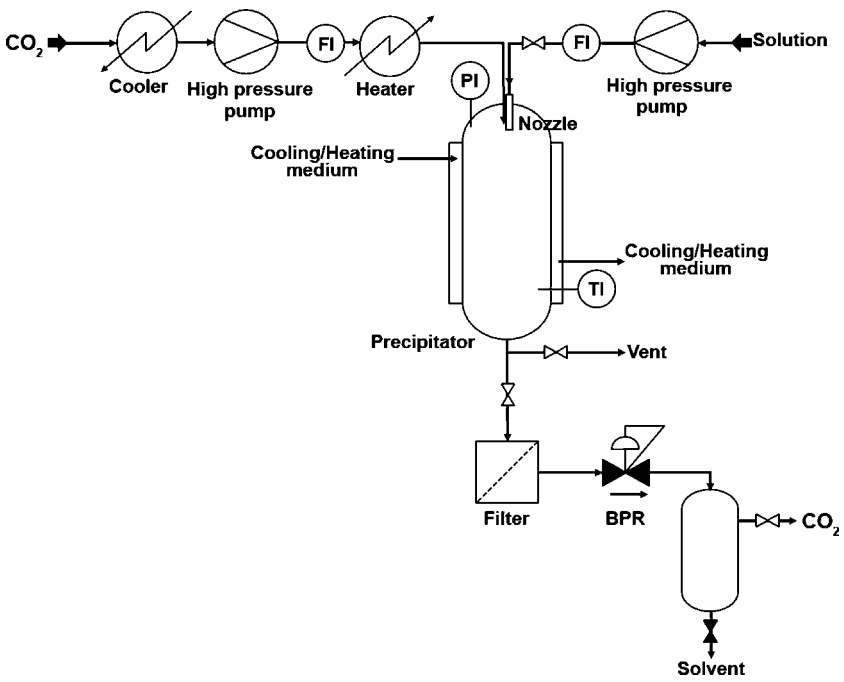

Fig. 1. Precipitation with compressed fluid antisolvent. BPR, back pressure regulator; PI, pressure indicator; TI, temperature indicator; FI, flow indicator.

significantly [18]. When T_m is depressed, the surface molecules of the precipitates have high molecular mobility and it results in the coalescence of nanoparticles. This phenomenon can actively occur especially in the amorphous materials that have high molecular mobility [15]. Second, weak interaction between solvent and antisolvent also induces the coalescence of the precipitates [2,19]; solvent absorbed by the precipitates reduces the viscosity of the powders [20]. In this case, the coalescence behavior can be reduced when solvent/antisolvent interaction is strong; an increase of pressure higher than 18 MPa reduced the coalescence of tetracycline at 313.15 K [19,1].

From this model, we expected that less coalesced precipitates could be obtained using liquid carbon dioxide as an antisolvent. Molecular mobility at the surface would be reduced at low temperatures. Furthermore, liquid CO_2 is entirely miscible with a variety of organic solvents [21], whereas supercritical carbon dioxide cannot be entirely miscible depending on concentration, pressure, and temperature. This dissimilarity in miscibility would affect the morphologies and crystal size [22].

Our goal of this study is divided into two parts. First, in order to test our hypothesis, we micronized a model compound using liquid and supercritical CO_2 in the precipitation with compressed fluid antisolvent (PCA) process. The model compound was tetracycline, a broad-spectrum antibiotic. Chu et al. (2009) and Reverchon et al. (1999) obtained tetracycline as coalesced microparticles in the SAS process [3,19]. They measured mean diameter of the precipitates and reported that significant coalescence occurred among the precipitates. However, they did not quantitatively characterize the degree of coalescence. They attempted to prevent the coalescence of nanoparticles by altering operating conditions and solvents. However, those changes only had little effects on the degree of coalescence.

In this work, scanning electron microscope (SEM) images were used to compare the morphologies of the precipitates. SEM images have been frequently used to understand the influences of process parameters on the coalescence behavior qualitatively [23,24]. In order to compare the degree of coalescence quantitatively, BET surface analysis was used to measure the specific surface area of the processed materials in this work. Second, we tested the hypothesis that solvent/antisolvent interaction mainly controls the coalescence behavior of tetracycline. To represent the solvent/antisolvent interaction quantitatively, Hansen solubility parameters (HSPs) were introduced to explain the phenomena observed in the precipitator and the degree of coalescence after the PCA process.

2. Theory

2.1. Hansen solubility parameter (HSP)

Hildebrand and his coworkers introduced the concept of solubility parameter [25]. It is defined as the square root of cohesive energy density:

$$\delta = \left(\frac{\Delta H_v - RT}{V}\right)^{1/2} \quad (1)$$

Table 1
Calculated HSPs and interaction distances.

P (MPa)	T (K)	δ_{d,CO_2} $(MPa)^{1/2}$	δ_{p,CO_2} $(MPa)^{1/2}$	δ_{h,CO_2} $(MPa)^{1/2}$	δ_{t,CO_2} $(MPa)^{1/2}$	$\delta_{d,DMF}$ $(MPa)^{1/2}$	$\delta_{p,DMF}$ $(MPa)^{1/2}$	$\delta_{h,DMF}$ $(MPa)^{1/2}$	$\delta_{t,DMF}$ $(MPa)^{1/2}$	R $(MPa)^{1/2}$
10	278.15	12.67	4.78	5.48	14.61	17.97	13.88	11.75	25.57	15.32
10	288.15	11.70	4.64	5.24	13.63	17.75	13.81	11.54	25.28	16.44
10	298.15	10.52	4.44	4.96	12.45	17.54	13.74	11.34	25.00	18.00
10	313.15	7.58	3.90	4.26	9.52	17.21	13.64	11.03	24.58	22.64
10	323.15	4.10	3.05	3.29	6.07	17.00	13.57	10.83	24.30	28.87
15	278.15	13.15	4.86	5.56	15.09	18.01	13.89	11.76	25.60	14.64
20	278.15	13.55	4.91	5.63	15.47	18.07	13.91	11.78	25.67	14.16
15	313.15	9.93	4.34	4.75	11.83	17.30	13.67	11.05	24.67	18.56
20	313.15	10.88	4.50	4.92	12.76	17.37	13.69	11.07	24.73	17.05